Semiclassical Dynamics Based on Quantum Trajectories

2 AUTHORS:

Sophya Garashchuk
University of South Carolina
55 PUBLICATIONS **763** CITATIONS

SEE PROFILE

Vitaly A Rassolov
University of South Carolina
80 PUBLICATIONS **7,321** CITATIONS

SEE PROFILE

Semiclassical dynamics based on quantum trajectories

Sophya Garashchuk *, Vitaly A. Rassolov

Department of Chemistry and Biochemistry, University of South Carolina, Columbia, SC 29208, USA

Abstract

We present a trajectory-based method that incorporates quantum effects in the context of Hamiltonian dynamics. It is based on propagation of trajectories in the presence of quantum potential within the hydrodynamic formulation of the Schrödinger equation. The quantum potential is derived from the density approximated as a linear combination of gaussian functions. One-gaussian fit gives exact result for parabolic potentials, as do successful semiclassical methods. The limit of the large number of fitting gaussians and trajectories gives the full quantum–mechanical result. The method is systematically improvable from classical to fully quantum, as demonstrated on a transmission through the Eckart barrier.

© 2002 Elsevier Science B.V. All rights reserved.

1. Introduction

Quantum dynamics is essential for understanding of a multitude of physical and chemical systems, exhibiting tunneling, interference, non-adiabatic behavior and other quantum–mechanical (QM) phenomena. Traditional methods of solving the time-dependent Schrödinger equation (SE) are based on spatial grids, basis sets of functions or discrete variable representation [1]. The numerical efforts for these exact QM methods scale exponentially with the dimensionality of a system. Despite many recent advances in theoretical and numerical approaches and in the computer facilities, the current state-of-the-art exact full-dimen-sional calculations in chemistry have been performed for a few four-atom systems. In contrast, methods of molecular dynamics, where a phase space ensemble of classical trajectories represents the density distribution of a localized wavefunction, are applicable to large systems of thousands of particles, like liquids and biomolecules. Molecular dynamics works well for nearly classical systems of heavy particles, but it is not capable of reproducing QM effects (for an example of a combined molecular dynamics/QM treatment see [2]). The exponential scaling of exact QM methods with the dimensionality and the importance of QM effects motivate development of new approaches, that combine the simplicity of classical dynamics with the rigor of quantum mechanics.

One class of alternative methods includes semiclassical (SC) methods, based on classical trajectories, each carrying a time-dependent phase and amplitude. The main advantage of SC meth-

---

* Corresponding author. Fax: +803-777-9521.

E-mail address: sgarashc@mail.chem.sc.edu (S. Garash-chuk).

ods is their local character and incorporation of some quantum effects. Most SC methods are based on the stationary phase approximation to SE in the limit of $\hbar \to 0$ or large mass, which is appropriate for studies of heavy particles such as nuclei in molecules. In the last several years the initial value representation methods [3], in particular the method of Herman and Kluk (HK) [4], have been developed and applied to a wide range of problems such as double-slit experiments, photo-detachment, reactive scattering, non-adiabatic and condensed phase dynamics (for instance, [5–9]). Among the drawbacks are the facts that these methods are formulated in phase space in terms of oscillatory integrals over trajectories, and that the inherent semiclassical error is difficult to assess and improve.

The second class of alternatives to traditional quantum dynamics is based on the so-called Bohmian or quantum trajectories (QT) that solve the hydrodynamic form of SE [10]. The wavefunction of a system is represented in a set of 'particles' that move according to the classical equation of motion and carry along certain density. The non-local QM character enters this formulation by means of the quantum potential (QP), which depends on the density and its derivatives. QP governs the dynamics of the 'particles' along with the classical external potential. Since solution of SE is based on trajectories, rather than grid points, the scaling bottleneck is avoided. In the last few years several practical ways of using quantum trajectories have been suggested, such as local least-square fit, adaptive and moving grids [11–14]; methodology of using QT within the Wigner representation, dissipative and non-adiabatic dynamics have been also developed [15–17]. Application to a few two- and three-dimensional model problems, where a small number of trajectories was sufficient, is encouraging. However, for general problems accurate implementation of the hydrodynamic SE, which is non-linear, at present, seems impractical. A simple examination of one-dimensional systems with a barrier [18] shows, that QP becomes a rapidly varying function of a large amplitude and is responsible for complicated and unstable dynamics of QTs, whenever the system undergoes drastic changes, such as a bifurcation. For example, analytical solution for the Eckart barrier [19] has numerically poor convergence, when used for propagation of QTs representing a bifurcating wavepacket. QTs were originally proposed for the purpose of interpretation [10] and were also used in the context of non-adiabatic dynamics as a theoretical [20] and a practical [21] tool with QP partly neglected.

Our goal is to use approximate quantum potential (AQP), rather then exact QP, which can be computed efficiently and will give accurate results for semiclassical systems. The central step is to fit the density in terms of gaussian functions globally. The fitted density is used to compute QP. The accuracy of the fit controls the degree in which semiclassical description approaches exact quantum dynamics. In addition, we avoid solution of the equation on wavefunction density, by treating weights of trajectories as constant in a course of dynamics. The formulation and the fitting procedure are outlined in Section 2, followed by an illustrative application and a discussion of Section 3. Section 4 concludes.

2. Description of quantum potential

The hydrodynamic form of SE is based on the ansatz

$$
\begin{aligned}
\psi(\mathbf{x}, t) &= A(\mathbf{x}, t) \exp\left(\frac{\imath}{\hbar} S(\mathbf{x}, t)\right) \\
&= \sqrt{\rho(\mathbf{x}, t)} \exp\left(\frac{\imath}{\hbar} S(\mathbf{x}, t)\right),
\end{aligned} \tag{1}
$$

where amplitude $A(\mathbf{x})$ and phase $S(\mathbf{x})$ are both real functions. After this substitution and a transformation into a moving frame of reference, SE becomes equivalent to a set of equations

$$
\frac{dS(\mathbf{x}, t)}{dt} = \frac{m\mathbf{v}^2}{2} - V - U, \tag{2}
$$

$$
\frac{d\rho(\mathbf{x}, t)}{dt} = -\nabla \cdot \mathbf{v}\rho(\mathbf{x}, t), \tag{3}
$$

where U,

$$
U = -\frac{\hbar^2}{2m} \frac{\nabla^2 A(\mathbf{x}, t)}{A(\mathbf{x}, t)}, \tag{4}
$$

is the non-local QP, and momentum is identified as $\mathbf{p} = m\mathbf{v} = \nabla S(\mathbf{x}, t)$. Eq. (2) is the Lagrangian equation for a particle of mass m moving under the influence of the classical potential V and the quantum potential U. Position and momentum of the particle, $\mathbf{x} = \mathbf{x}(t)$ and $\mathbf{p} = \mathbf{p}(t)$, define a quantum trajectory and can be found from Hamilton's equations of motion. Eq. (1) implies that $\rho(\mathbf{x}(t), t)$ remains a single valued function at all times, i.e., the quantum trajectories do not cross. After initial discretization of the density in a set of particles, a certain amount of density within a volume element $\delta\Omega(t) = \delta x^{(1)}(t)\delta x^{(2)}(t)\delta x^{(3)}(t) \cdot \ldots$ is associated with each trajectory and this quantity, its weight w, is conserved (as follows from the equation of continuity, Eq. (3)),

$$\rho(\mathbf{x}_i, t)\delta\Omega_i(t) = w_i. \tag{5}$$

The conservation of the total density, i.e., the wavefunction normalization, is

$$\sum_i \rho(\mathbf{x}_i, t)\delta\Omega_i(t) = \sum_i w_i = 1. \tag{6}$$

The transmission of a wavepacket through a barrier (from the reactant to product region), which is the simplest case of reactive scattering, is expressed in terms of the weights

$$P(t) = \sum_{i,\text{prod}} w_i(\mathbf{x}_i, t), \tag{7}$$

where only the weights of trajectories that reached the product region are included in the sum. In the example below we will consider the phase-independent quantities, density and probability. We also explicitly use Eq. (5): weight w_i associated with each trajectory remains constant in a course of dynamics. Therefore, we do not need to solve the continuity equation (3) to determine $\rho(\mathbf{x}, t)$.

At each propagation time step, we approximate the density $\rho(x)$, which is positive and localized, in terms of gaussian functions $g_n = \exp(-a_n^2(x - X_n)^2)$ as (omitting t in the argument)

$$\rho(x) \approx f(x) = \sum_n c_n^2 g_n. \tag{8}$$

The approximation can be of arbitrary high accuracy and is non-unique due to over-completeness of gaussian basis. The fitting procedure is outlined for one-dimensional case; the multidimensional generalization is straightforward. We find a set of g_n's, i.e., their overall number and their parameters $s = \{c_1, X_1, a_1, c_2, X_2, a_2, \ldots\}$, from the minimization of F,

$$F = \int (\rho(x) - f(x))^2 \, dx, \tag{9}$$

by solving a set of equations for its gradient $\mathbf{G}$

$$G_n = \frac{\partial F}{\partial s_n} = -2 \int \rho(x) \frac{\partial f(x)}{\partial s_n} \, dx$$
$$+ 2 \int \frac{\partial f(x)}{\partial s_n} f(x) \, dx = 0. \tag{10}$$

Note, that $\rho(x)$ appears only in the first integral in combination with dx and can be replaced with w_i for discrete trajectories. Thus, in the fitting procedure $\rho(x)$ is not required explicitly. We solve Eq. (10) by iterative quadratic technique with the full matrix of second derivatives [22], taking advantage of their analytical form. For propagation of a gaussian wavepacket, the fitting starts with a single g_1, and the number of fitting gaussians is increased each time, when F exceeds a small constant, up to a maximum number of g_n's, N.

Discretization of the initial wavefunction gives us $\rho(x)$ only at the position of trajectories x_i. We find that the fitting can be done much more easily, if instead of $\rho(x)$ we work with the the convoluted density $\tilde{\rho}(x)$, which is defined for all x,

$$\tilde{\rho}(x) = \sqrt{\frac{\beta}{\pi}} \int \exp\left(-\beta(x - x_i)^2\right) \rho(x_i) \, dx_i$$
$$= \sum_i \exp\left(-\beta(x - x_i)^2\right) w_i. \tag{11}$$

Here and below tilde symbol designates quantities referred to a convolution. Summation goes over all trajectories. The fit to the original density $\rho(x)$ can be rigorously restored, provided the fitting gaussians $\tilde{g}_n$ are wider than the convolution gaussian. Eq. (9) becomes

$$\tilde{F} = \sqrt{\frac{2\beta}{\pi}} \sum_{ij} \exp\left(-\frac{\beta}{2}(x_i - x_j)^2\right) w_i w_j$$
$$- 2 \int \tilde{\rho}(x)\tilde{f}(x) \, dx + \int \tilde{f}(x)^2 \, dx, \tag{12}$$

where all the integrals are analytical. As easy to see, our formulation of the fitting procedure using weights $\{w_i\}$, is formally insensitive to the crossing of trajectories with approximate QP. Note, that the only term, containing a double sum over trajectories in Eq. (12), is not actually needed to solve the convoluted version of Eq. (10), $\tilde{\mathbf{G}} = 0$. The double sum is only required to check that we have enough gaussians in the fit and that F is sufficiently small. Moreover, in a SC regime of a few g_n's in Eq. (8), β can be chosen very large. Strong cutoffs can be imposed on the double sum in Eq. (12) to make evaluation of $\tilde{F}$ linear with the number of trajectories.

The original fit $f(x)$ is obtained, if we treat g_n as being convoluted in the same way as $\rho(x)$. The relation between the convoluted and original parameters, $a_n^2 = \tilde{a}_n^2 z$ and $c_n^2 = \tilde{c}_n^2 \sqrt{z}$ with $z = \beta/(\beta - \tilde{a}_n^2)$, imposes the restriction on the width of $g_n : \tilde{a}_n^2 < \beta$. In practice, for $\tilde{f}(x)$ we include g_n's that satisfy this condition, by assuming $\tilde{a}_n^2 = \beta/(\Delta + \alpha_n^2), \Delta > 1$. In application below, one or two iterations were sufficient to update $\tilde{f}(x)$ taken from the previous time step, if the number of g_n's did not change, and 5–20 iterations otherwise.

3. Results and discussion

Now let us consider a scattering of a wavepacket, using the AQP method. The initial wavepacket, $\psi(x,0) = \exp(-\gamma(x - q_0)^2 + \imath p_0(x - q_0))(2\gamma/\pi)^{1/4}$, is located on the left of the Eckart barrier, $V(x) = D/\cosh^2(\lambda x)$. The parameters of the barrier, $D = 16.0$ and $\lambda = 1.3624$ for $m = 1$, mimic hydrogen exchange reaction. Parameters are given in atomic units, scaled by $m_H/2$. We look at the probability of transmission of the wavepacket to the right of the barrier, as a function of the initial energy of the wavepacket $E = \gamma/2 + p_0^2/2$,

$$P(E) = \int_0^\infty \rho(x,t)\,\mathrm{d}x = \lim_{t \to \infty} P(t). \tag{13}$$

$P(t)$ is given by Eq. (7). Parameters of the initial wavepacket are $\gamma = 6$ and $q_0 = -2$. Tunneling in this system is strong, but the system can be viewed as semiclassical in a sense that the classical limit of SE gives a reasonable answer – a step-function for $P(E)$. The error of AQP probabilities, computed with the maximum number of g_n's $N = 1$, $N = 2$ (199 trajectories) and $N = 12$ (799 trajectories) and with the semiclassical HK method are presented on Fig. (1). Classical ($N = 0$) and QM probabilities are shown on the insert. As one can see, a one-gaussian fit reproduces QM results very well, and an increase in the number of the fitting gaussians improves this agreement. A general feature of the AQP method is that a single gaussian fit gives exact time-evolution of a gaussian wavepacket in a parabolic potential. We also find it very encouraging, that the quality of a one-gaussian approximation is about the same as for the most widely used semiclassical HK method, that required in this case ten times more trajectories and $4N_{\text{traj}}^2$ auxiliary equations for the stability analysis. The similarity of the results obtained with HK method and a few-gaussian AQP is not accidental. In the process of reconstruction of the wavefunction, contribution of a quantum trajectory depends on the volume element $\delta\Omega(t)$ and on the phase $S(x,t)$, in analogy to the stability prefactor and action of the classical trajectories in HK method. One of the effects of QP is to spread the trajectories in energy, which is well reproduced even with a single-gaussian AQP. This effect is analogous to the phase space sampling of the classical trajectories in HK method. More detailed analysis on the relation between AQP and HK method will be given in the forthcoming publication.

The results of a more accurate calculation are presented on Fig. (2), showing a bifurcation of the wavepacket with initial momentum $p_0 = 6$ on the barrier in comparison to QM results. The density was fitted with the maximum of $N = 8$ g_n's and 399 trajectories. Note, that for $t = 0.8$ we see an additional small amplitude lobe beginning to form at the front of the reflected wavepacket. It is caused by the interference of the incoming and reflected components of $\psi(x,t)$, and it is not accurately reproduced for longer times with the limited number of g_n's. As expected, interference effects are more sensitive to the quality of the approximated density, then the probability found in a phase-insensitive way, Eq. (13). The bifurcation itself is described quite well. In general, for AQP method
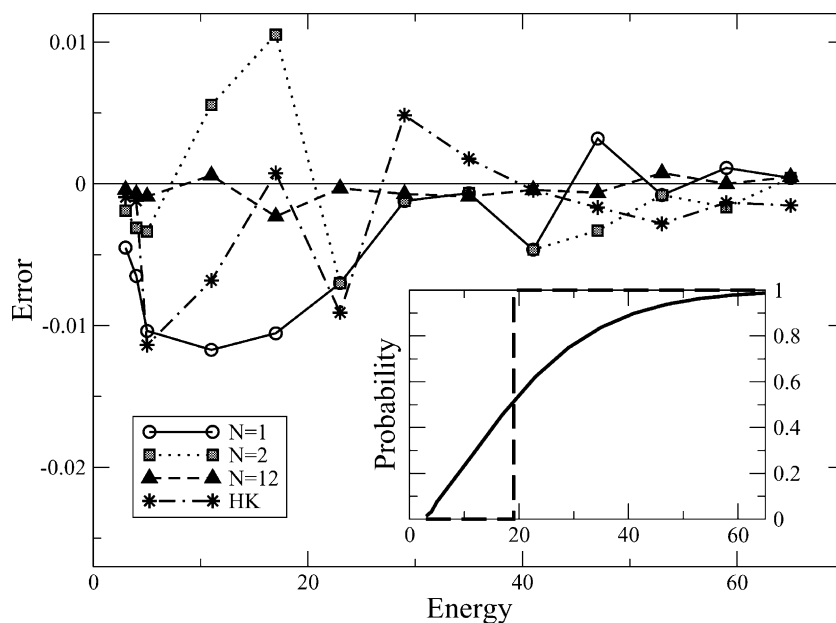
Fig. 1. Difference of the transmission probability for AQP with the maximum of $N = 1$, 2, 12 fitting gaussians and for HK semiclassical propagator with the QM result. QM (solid line) and classical ($N = 0$, dashed line) probabilities are shown on the insert.
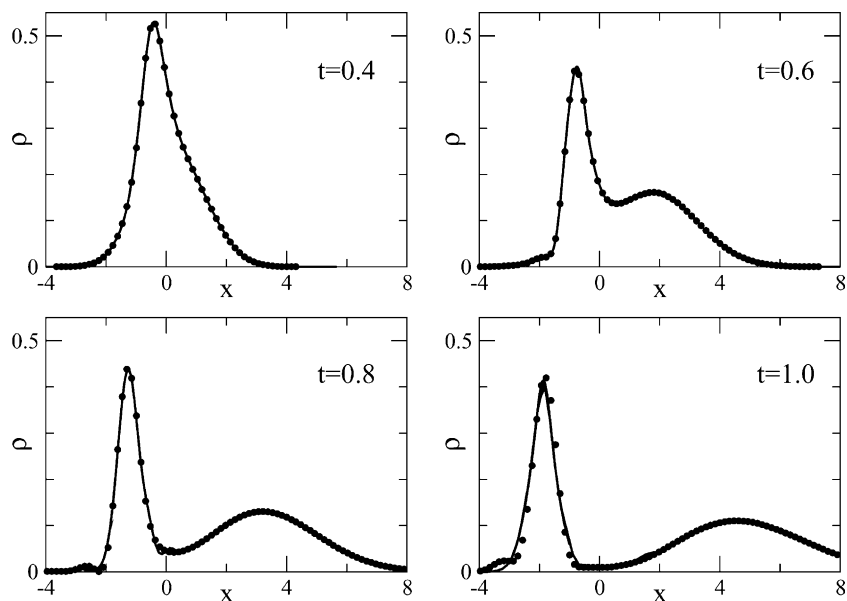

Fig. 2. Density $\rho(x, t)$ of a bifurcating wavepacket for $t = 0.4$, 0.6, 0.8, 1.0; AQP density for $N = 8$ and QM density are shown with a solid line and circles, respectively.

numerical efforts scale linearly with the number of trajectories. The cost of a few-gaussian optimization is small compared to a multidimensional trajectory propagation. Quantum trajectories must be propagated simultaneously, unlike in HK method, but they sample just the coordinate and not the phase space, and do not require expensive stability analysis.

4. Conclusions

We have described a new approach to approximation of quantum dynamics. Our method is based on trajectory propagation in the presence of approximate quantum potential, and it has full QM as a limit of highly accurate QP and many trajectories. By using constant in time weights for the trajectories, we avoid the explicit solution of the continuity equation for density. QP is determined from a global fit of the density in terms of gaussian functions. One-gaussian approximation is exact for a gaussian wavepacket in any parabolic potential, and we have shown that it also gives good description of tunneling in a one-dimensional open system. We expect that a few-gaussian (perhaps, one function per channel) AQP will give an adequate description of semiclassical systems, such as in reactive scattering of molecules, and, being systematically improvable and cheaper, will be superior to the initial value representation semiclassical methods. Currently, we are working on phase approximations, that are consistent with the density approximations, and on application of AQP to multidimensional reactive scattering.

References

[1] J.C. Light, T. Carrington Jr., Adv. Chem. Phys. 114 (2000) 263.
[2] V. Guallar, D.L. Harris, V.S. Batista, W.H. Miller, J. Am. Chem. Soc. 124 (2002) 1430.
[3] W.H. Miller, J. Phys. Chem. A 105 (2001) 2942.
[4] M. Herman, E. Kluk, Chem. Phys. 91 (1984) 27.
[5] R. Gelabert, X. Gimenez, M. Thoss, H.B. Wang, W.H. Miller, J. Chem. Phys. 114 (2001) 2572.
[6] M.L. Brewer, J.S. Hulme, D.E. Manolopoulos, J. Chem. Phys. 106 (1997) 4832.
[7] S. Garashchuk, D.J. Tannor, Chem. Phys. Lett. 262 (1996) 477.
[8] F. Grossmann, Phys. Rev. A 60 (1999) 1791.
[9] K. Thomson, N. Makri, J. Chem. Phys. 110 (1999) 1343.
[10] D. Bohm, Phys. Rev. 85 (1952) 167.
[11] C.L. Lopreore, R.E. Wyatt, Phys. Rev. Lett. 82 (1999) 5190.
[12] R.E. Wyatt, E.R. Bittner, J. Chem. Phys. 113 (2000) 8898.
[13] D. Nerukh, J.H. Frederick, Chem. Phys. Lett. 332 (2000) 145.
[14] B.K. Dey, A. Askar, H. Rabitz, J. Chem. Phys. 109 (1998) 8870.
[15] A. Donoso, C.C. Martens, J. Chem. Phys. 115 (2002) 6309.
[16] E.R. Bittner, J. Chem. Phys. 115 (2002) 6309.
[17] R.E. Wyatt, C.L. Lopreore, G. Parlant, J. Chem. Phys. 114 (2001) 5113.
[18] P.R. Holland, The Quantum Theory of Motion, Cambridge University Press, Cambridge, 1993.
[19] C. Eckart, Phys. Rev. 35 (1930) 1303.
[20] J.C. Burant, J.C. Tully, J. Chem. Phys. 112 (2000) 6097.
[21] E. Gindensperger, C. Meier, J.A. Beswick, J. Chem. Phys. 113 (2000) 9369.
[22] P. Pulay, J. Comp. Chem. 3 (1982) 556.